

## **ANALYSIS OF DISPERSION RELATION OF PIECEWISE LINEAR RECURSIVE CONVOLUTION FDTD METHOD FOR SPACE-VARYING PLASMA**

**X. Ai**

Science and Technology on Antenna and Microwave Laboratory  
Xidian University, Xi'an, Shaanxi 710071, China

**Y.-P. Han and C.-Y. Li**

School of Science  
Xidian University, Xi'an, Shaanxi 710071, China

**X.-W. Shi**

Science and Technology on Antenna and Microwave Laboratory  
Xidian University, Xi'an, Shaanxi 710071, China

**Abstract**—The dispersion relation of piecewise linear recursive convolution finite difference time domain (PLRC-FDTD) method for space-varying plasma is analyzed using a novel equivalent method. The equivalent dispersion and dissipation errors have been taken into account. The efficiency of the novel equivalent method is substantiated by computing the test and reference transmitted electric field. The comparison of the test and reference solutions validates that the equivalent method is an efficient method to analyze the dispersion relation of PLRC-FDTD method used for space-varying plasma.

### **1. INTRODUCTION**

Over the past few years, a number of finite difference time-domain (FDTD) [1–15] methods have been used to model electromagnetic wave interaction with unmagnetized and magnetized cold plasma. These methods include the recursive convolution (RC) method [2], which becomes piecewise linear recursive convolution (PLRC) method [3] for

more precision, the auxiliary differential equation (ADE) methods [4], and current density recursive convolution (JEC) method [5]. These are mainly used to model the uniform plasma, but also used to simulate the nonuniform plasma [6, 7]. Due to the accuracy and stability [8, 9], the PLRC-FDTD method is more suitable than the other methods for simulating the unmagnetized plasma.

Actually, in many cases, the permittivity of cold plasma is not a constant at different spatial locations, such as the reentry bodies coated with plasma sheath and the nonuniform plasma be used for improving the properties of antenna [10]. Therefore, analyzing the numerical dispersion caused by the permittivity varies with space is of significant value. Although the stability and accuracy of the PLRC-FDTD method for uniform plasma were demonstrated in [9], the numerical dispersion for nonuniform plasma which defined as space-varying plasma in [6] has not been considered.

To analyze the accuracy of PLRC-FDTD method for space-varying plasma, in this paper, we introduce a equivalent method to analyze the dispersion relation of PLRC-FDTD method at a fixed angular frequency for all different cells in Yee space. The equivalent dispersion relation has been separated into two parts: the dispersion and dissipation errors, which control the phase and the amplitude errors, respectively. The efficiency of the novel method is confirmed by comparing the test and reference solution to transmitted electric field in one-dimensional case.

## 2. METHODOLOGY

Assuming the propagation direction is in  $z$ -axis, in one-dimensional case, the general form of PLRC-FDTD update equation scheme is given by [3]. Generally, the plasma frequency  $\omega_p$  can be the expression as follow:

$$\omega_p^2 = \frac{n_e e^2}{m_e \epsilon_0} \quad (1)$$

where  $e$  and  $m_e$  are the electric quantity and mass of a unity electron respectively,  $n_e$  is the electron density.

However, in many cases, the electron density of plasma is not only a constant, but also varies with spatial locations, which can be defined as:

$$n_e(\vec{r}) = n_0 f(\vec{r}) \quad (2)$$

where  $n_0$  is the saturation electron density at the location  $\vec{r} = r_0$ ,  $\vec{r}$  is the location vector and  $f(\vec{r})$  is the electron density profile.

Obviously, for space-varying plasma, the plasma frequency  $\omega_p$  is a function of location, which can be defined as  $\omega_p(\vec{r})$

$$\omega_p^2(\vec{r}) = \frac{n_e(\vec{r})e^2}{m_e\varepsilon_0} \quad (3)$$

where  $n_e(\vec{r})$  is the same as (2),  $e$  and  $m_e$  are the same as (1).

It should be pointed out that the PLRC-FDTD scheme for uniform plasma taking the constant  $\omega_p$  into account, but for space-varying plasma taking the variable  $\omega_p(\vec{r})$  into account, which is the only difference between the two applications of PLRC-FDTD scheme.

However, the space-varying plasma should be considered as a multilayered medium. Therefore, the properties of PLRC-FDTD scheme for space-varying plasma could be analyzed via a equivalent method. As accuracy is a key characteristic of FDTD method, a useful way to determine the accuracy of FDTD method is to analyze the dispersion relation. The dispersion relation satisfied by the finite-difference approximations is found by assuming  $e^{j(\omega n\Delta t - k_{num}m\Delta z)}$  variation for the field quantities.  $n$  and  $m$  are the time step and spatial cell point, respectively, and the propagation direction is in  $z$ -axis. Then the dispersion relation for PLRC-FDTD method in one-dimensional case is given in [9], and for space-varying plasma, it can be rewritten as follows:

$$\left(\frac{c_0\Delta t}{\Delta z}\right)^2 \sin^2(K_i\Delta z/2) = (1 - \xi_i^0) \sin^2\left(\frac{\omega\Delta t}{2}\right) + \frac{1}{4}\chi_i^0(1 - \exp(j\omega\Delta t)) - \frac{\frac{1}{4}\Delta\chi_i^0(1 - \exp(j\omega\Delta t)) - \Delta\xi_i^0 \sin^2\left(\frac{\omega\Delta t}{2}\right)}{\exp(j\omega\Delta t) - \exp(-v_c\Delta t)} \quad (4)$$

where  $\omega$  is the operating angular frequency, and the expressions for  $\xi_i^0$ ,  $\Delta\xi_i^0$ ,  $\chi_i^0$  and  $\Delta\chi_i^0$  are presented in [11] as a function of the plasma frequency  $\omega_p^2(\vec{r})$  and the collision frequency  $v_c$ .  $K_i$  is the numerical wave number.

Since the expression for the complex wave number cannot be given analytically, the dispersive relation in space-varying plasma cannot conveniently be expressed in terms of operating angular frequency and plasma medium parameters. Therefore, it appears to be more appropriate to present equivalent numerical wave numbers, which is similar to the method in [12]. For all the different cells at a fixed angular frequency  $\omega$ , the equivalent numerical wave number  $K_{eff}$  is defined as the average of the numerical wave number of each cell with  $K_i$  as a function of  $\omega_{p,i}^2$  which is the Yee algorithm form of  $\omega_p^2(\vec{r})$  and

the saturation electron density  $n_0$

$$K_{eff} = \frac{\sum_{i=1}^m K_i \omega_{p,i}^2}{\sum_{i=1}^m \omega_{p,i}^2} \quad (5)$$

The analytic plasma dispersion relation is

$$c^2 k^2 = \omega^2 - \frac{\omega_p^2}{1 - j \frac{v_c}{\omega}} \quad (6)$$

where  $c$  is the velocity of light in vacuum;  $\omega$  is the operating angular frequency;  $\omega_p$  is the plasma frequency;  $v_c$  is the collision frequency;  $j$  is  $\sqrt{-1}$ ; and  $k$  is the analytic wave number. For space-varying plasma being concerned about, the Equation (6) can be rewritten as follow:

$$c^2 k_i^2 = \omega^2 - \frac{\omega_{p,i}^2}{1 - j \frac{v_c}{\omega}} \quad (7)$$

where the  $\omega_{p,i}^2$  is the same as in (5), and  $c$ ,  $\omega$ ,  $v_c$ ,  $j$  are the same as in (6).

Similar to the numerical wave number, the analytic wave number of space-varying plasma is not a constant at a fixed angular frequency  $\omega$ . Therefore, a method should be used to determine the equivalent analytic wave number, as follow:

$$k_{eff} = \omega_{p,i}^2 \frac{\partial k(\omega, \omega_p^2)}{\partial (\omega_p^2)} \quad (8)$$

where  $\omega_{p,i}^2$  is just defined in Equation (3).

### 3. NUMERICAL RESULTS

Now that both the equivalent numerical wave number and equivalent analytic wave number have been derived, to bring to light the equivalent dispersion errors introduced by the PLRC-FDTD scheme for one-dimensional space-varying plasma, which have different distribution profiles, it is more expressive to consider and plot the following relative error functions:

$$e_{real} = \left| \frac{\text{Re} \{k_{eff} - K_{eff}\}}{\text{Re} \{k_{eff}\}} \right| \quad (9)$$

and

$$e_{imag} = \left| \frac{\text{Im} \{k_{eff} - K_{eff}\}}{\text{Im} \{k_{eff}\}} \right| \quad (10)$$

where  $K_{eff}$  and  $k_{eff}$  are the solution to (5) and (8).

Obviously,  $e_{real}$  is a measure of the equivalent numerical phase error, which controls the phase error of each frequency, called equivalent dispersion error, and  $e_{imag}$  is a measure of the equivalent numerical attenuation error, which controls the amplitude error of each frequency, called equivalent dissipation error.

The one-dimensional computational space consists of 800 spatial cells each 30 m thick ( $dz = 30$  m), with the plasma slab occupying cells 300 through 500. The time step is  $0.05 \mu\text{s}$  ( $dt = 0.5dz/c$ ). Herein, four kinds of electron density profile  $f(\vec{r})$  were considered as follows:

$$f_{linear}(\vec{r}) = \frac{\vec{r}}{d} \quad (11)$$

$$f_{parabola}(\vec{r}) = \left(\frac{\vec{r}}{d}\right)^2 \quad (12)$$

$$f_{\sin e}(\vec{r}) = \sin\left(\frac{\pi\vec{r}}{2d}\right) \quad (13)$$

$$f_{epstein}(\vec{r}) = \frac{1}{1 + \exp\left(-\frac{\vec{r}-d/2}{\sigma}\right)} \quad (14)$$

where  $\vec{r}$  is the location vector, in one-dimensional case,  $\vec{r} = \vec{z}$ ;  $d$  is the thickness of the plasma; and  $\sigma$  is density scale length,  $\sigma = 10dz$ .

Then plasma frequency  $\omega_p(\vec{r})$  can be derived using (2) and (3) at all cells in Yee space and for different kinds. The plasma parameter values for the simulation are chosen as the saturation electron density  $n_0 = 2.83 \times 10^9 \text{ m}^{-3}$ , and the corresponding max plasma frequency  $\omega_p = 3 \times 10^6 \text{ rad/s}$ , the collision frequency  $\nu_c = 3.0 \times 10^7 \text{ Hz}$ . Figure 1 shows the curves of the electron density of different distribution functions versus cell numbers.

The equivalent dispersion error and the equivalent dissipation error versus the operating angular frequency for the above plasma parameter values have been shown in Figures 2 and 3. In the range of  $\omega = 10^4 - 5 \times 10^6 \text{ rad/s}$ , among the four kinds of distribution profile, the equivalent dispersion has the lowest peak near  $\omega = 2 \times 10^5 \text{ rad/s}$ , and this is mainly due to the corresponding plasma frequency of the space-varying plasma, which could be obtained via the mathematical expectation of the electron density. The equivalent dispersion of Epstein distribution profile is larger than others, probably because the derivative of the Epstein distribution profile function is not strictly monotony. The equivalent dissipation for the four kinds of distribution profile is closed to each other. For all of the distribution profiles, the lowest equivalent dispersion and dissipation error are below the max

plasma frequency. Therefore, most of the errors in a real simulation would come from frequencies near and above the plasma frequency.

Finally, the numerical experiments of the different distribution profiles to substantiate the analysis of equivalent dispersion and dissipation errors are presented. As the analysis above is based on errors as a function of temporal frequency, we will examine the phase

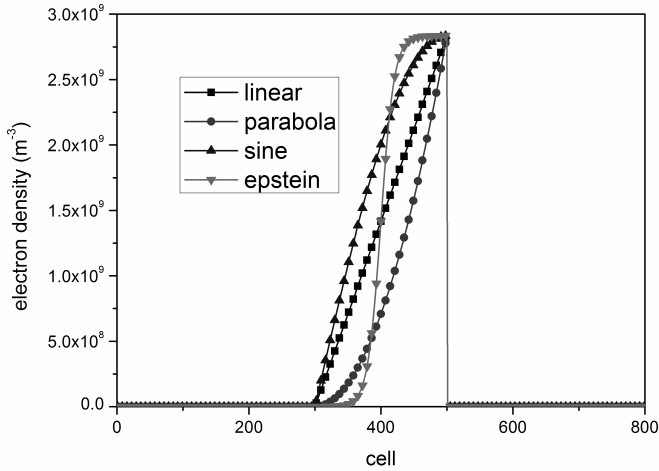


**Figure 1.** Electron density distribution.

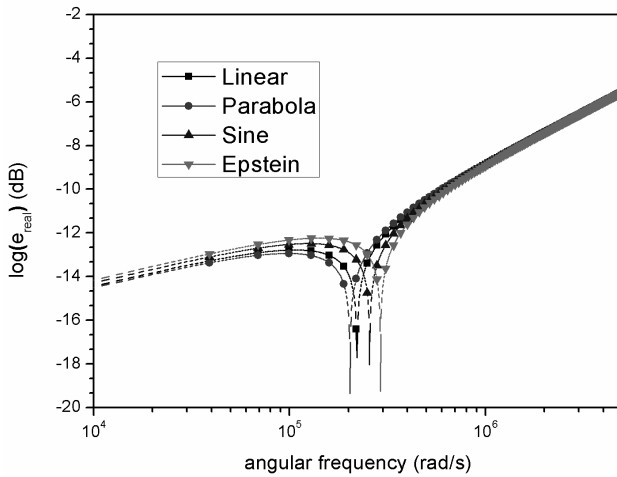


**Figure 2.** Equivalent dispersion error versus operating frequency.

and amplitude of transmitted electric field as function of temporal frequency, too. The calculation parameter values used for test solution to each kind of the distribution are the same as above used. The reference solutions to each kind of distribution profile could be obtained through setting  $dt = dz/c$  (the magic time-step as described in [1]). When simulation running, this setting guarantees the stability and consistency of the FDTD method convergence to the exact solution, and the other calculation parameter values are maintained the same as those used for the test solution.

For each problem, a unity amplitude Gaussian pulse propagating in free space is used as incident wave. The pulse width is such that the spectral amplitude of the pulse is down by a factor of 100 (compared to the zero frequency amplitude) at  $\omega = 5 \times 10^6$  rad/s, and the plasma parameters remain the same as afore mentioned. Figure 4 shows the model of the calculation region. The transmitted electric field is sampled each time step at the cell 501, and the total

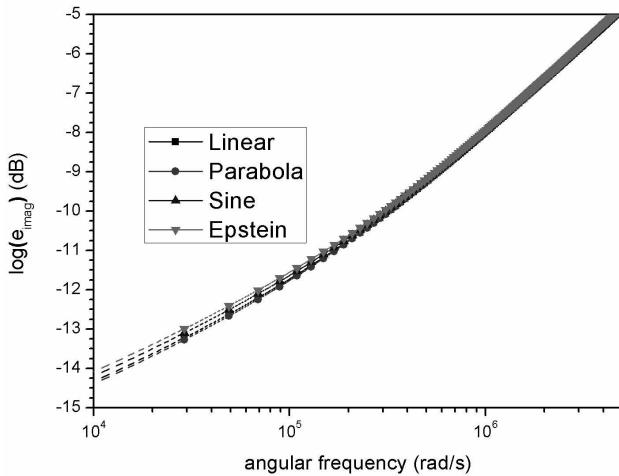


**Figure 3.** Equivalent dissipation error versus operating frequency.

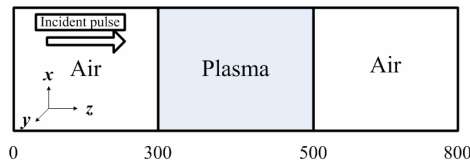


**Figure 4.** Model of the calculation region.

time step is chosen as 1000 to eliminate the error due to the outer grid boundary reflections. To get the phase and amplitude of the transmitted electric field, the fields versus time data were transformed to the frequency domain using discrete Fourier transform (DFT). Therefore, the test and reference complex solution to transmitted electric field for each distribution error between the test and reference solution can be separated into two parts: the phase error and the amplitude error. Figures 5 and 6 show the phase and the amplitude error-size relationship between various kinds of distribution profile. For perspective, the range  $\omega = 10^5 - 5 \times 10^6$  rad/s is chosen. The phase errors (controlled by the dispersion error) of transmitted electric fields for different distributions reach the highest peak near  $\omega = 10^5$  rad/s for all kinds of distribution profiles, and above  $\omega = 3 \times 10^5$  rad/s, the phase error for the Epstein distribution profile is lower than the others, corresponding to the error-size relationship results shown in Figure 2. The amplitude errors (controlled by the dissipation error) of transmitted electric field for different distribution profiles are fairly close to each other, corresponding to the error-size relationship results shown in Figure 3.

It can be seen that all of the above discussed results have a general agreement with the results shown in Figures 2 and 3 which demonstrate equivalent dispersion error and dissipation error, respectively.

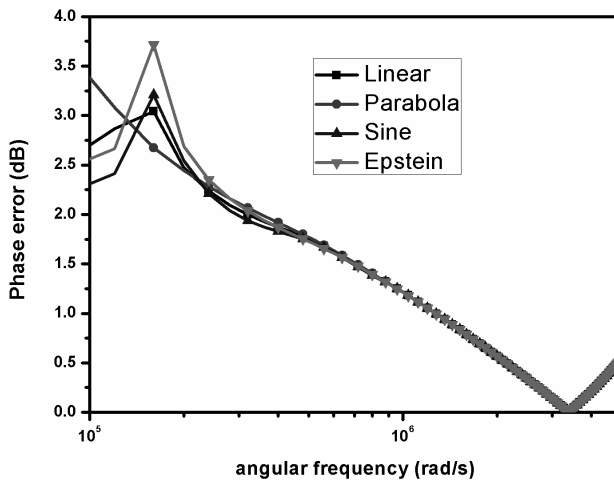


**Figure 5.** Error of phase for each kind of distribution profile.

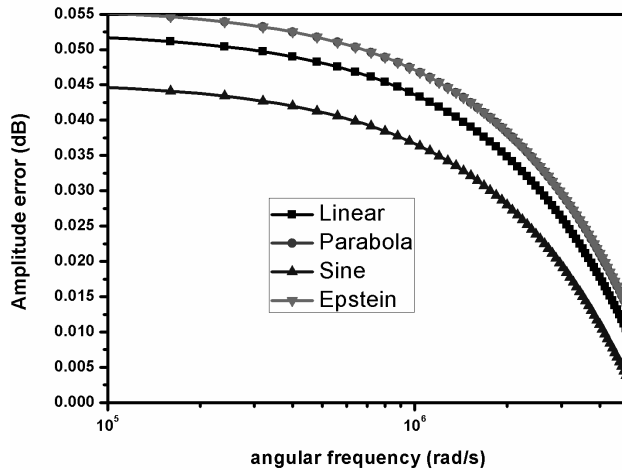


**Figure 6.** Error of amplitude for each kind of distribution profile.

#### 4. CONCLUSION

In this paper, a novel method to analyze the dispersion relation of PLRC-FDTD for space-varying plasma is derived. This method is based on the existing dispersion relation of PLRC-FDTD and equivalent theory. The equivalent dispersion relation for various distribution profiles has been calculated and compared, and the distribution profile that yields the lowest dispersion and dissipation errors has been analyzed. The numerical results indicate that the novel method is efficient enough to analyze the dispersion relation of PLRC-FDTD for space-varying plasma. However, it should be pointed out that because the collision frequency is a function of temperature, pressure and electron density, etc., taking account of the effect of collision frequency should be complicated. Therefore, the effect of collision frequency distribution has not been considered in the paper, and the effect would be studied in the future work.

#### ACKNOWLEDGMENT

This project is supported by the the National Science Foundation of China under Grant 60801039.

## REFERENCES

1. Taflove, A. and S. C. Hagness, *Computational Electromagnetics: Finite-difference Time-domain Method*, Artech House, Boston, MA, 2005.
2. Luebbers, R. J., F. Hunsberger, and K. S. Kunz, "A frequency-dependent finite-difference time-domain formulation for transient propagation in plasma," *IEEE Trans. on Antennas and Propagation*, Vol. 39, 29–34, 1991.
3. Kelley, D. F. and R. J. Luebbers, "Piecewise linear recursive convolution for dispersive media using FDTD," *IEEE Trans. on Antennas and Propagation*, Vol. 44, 792–797, 1996.
4. Young, J. L., "A full finite difference time domain implementation for radio wave propagation in a plasma," *Radio Sci.*, Vol. 29, 1513–1522, 1994.
5. Chen, Q., M. Katsurai, and P. H. Aoyagi, "An FDTD formulation for dispersive media using a current density," *IEEE Trans. on Antennas and Propagation*, Vol. 46, 1739–1746, 1998.
6. Lee, J. H. and D. K. Kalluri, "Three-dimensional FDTD simulation of electromagnetic wave transformation in a dynamic inhomogeneous magnetized plasma," *IEEE Trans. on Antennas and Propagation*, Vol. 47, 1146–1151, 1999.
7. Han, Z., J. Ding, P. Chen, Z. Zhang, and C. Guo, "FDTD analysis of three-dimensional target covered with inhomogeneous unmagnetized plasma," *2010 International Conference on Microwave and Millimeter Wave Technology (ICMMT 2010)*, 125–128, Piscataway, NJ, USA, May 8–11, 2010.
8. Young, J. L., A. Kittichartphayak, Y. M. Kwok, and D. Sullivan, "On the dispersion errors related to (FD)<sup>2</sup>TD type schemes," *IEEE Trans. on Microwave Theory and Techniques*, Vol. 43, 1902–1910, 1995.
9. Cummer, S. A., "An analysis of new and existing FDTD methods for isotropic cold plasma and a method for improving their accuracy," *IEEE Trans. on Antennas and Propagation*, Vol. 45, 392–400, 1997.
10. Li, X.-S. and B.-J. Hu, "FDTD analysis of a magneto-plasma antenna with uniform or nonuniform distribution," *IEEE Antennas and Wireless Propagation Lett.*, Vol. 9, 175–178, 2010.
11. Qian, Z. H., R. S. Chen, K. W. Leung, and H. W. Yang, "FDTD analysis of microstrip patch antenna covered by plasma sheath," *Progress In Electromagnetics Research*, Vol. 52, 173–183, 2005.
12. Christ, A., J. Frohlich, and N. Kuster, "Correction of numerical

- phase velocity errors in nonuniform FDTD meshes,” *IEICE Trans. on Communications*, Vol. 85, 2904–2915, 2002.
13. Wei, B., S.-Q. Zhang, Y.-H. Dong, and F. Wang, “A general FDTD algorithm handling thin dispersive layer,” *Progress In Electromagnetics Research B*, Vol. 18, 243–257, 2009.
  14. Atteia, G. E. and K. F. A. Hussein, “Realistic model of dispersive soils using PLRC-FDTD with applications to GPR systems,” *Progress In Electromagnetics Research B*, Vol. 26, 335–359, 2010.
  15. Heh, D. Y. and E. L. Tan, “Dispersion analysis of FDTD schemes for doubly lossy media,” *Progress In Electromagnetics Research B*, Vol. 17, 327–342, 2009.